

Journal Pre-proof

Efficient suppression of NRAS-driven melanoma by co-inhibition of ERK1/2 and ERK5 MAPK pathways

Christian Adam, Lorenza Fusi, Neele Weiss, Simon G. Goller, Katharina Meder, Verena G. Frings, Hermann Kneitz, Matthias Goebeler, Roland Houben, David Schrama, Marc Schmidt

PII: S0022-202X(20)31407-X

DOI: <https://doi.org/10.1016/j.jid.2020.03.972>

Reference: JID 2439

To appear in: *The Journal of Investigative Dermatology*

Received Date: 25 October 2019

Revised Date: 24 February 2020

Accepted Date: 18 March 2020

Please cite this article as: Adam C, Fusi L, Weiss N, Goller SG, Meder K, Frings VG, Kneitz H, Goebeler M, Houben R, Schrama D, Schmidt M, Efficient suppression of NRAS-driven melanoma by co-inhibition of ERK1/2 and ERK5 MAPK pathways, *The Journal of Investigative Dermatology* (2020), doi: <https://doi.org/10.1016/j.jid.2020.03.972>.

This is a PDF file of an article that has undergone enhancements after acceptance, such as the addition of a cover page and metadata, and formatting for readability, but it is not yet the definitive version of record. This version will undergo additional copyediting, typesetting and review before it is published in its final form, but we are providing this version to give early visibility of the article. Please note that, during the production process, errors may be discovered which could affect the content, and all legal disclaimers that apply to the journal pertain.

© 2020 The Authors. Published by Elsevier, Inc. on behalf of the Society for Investigative Dermatology.



**Efficient suppression of NRAS-driven melanoma by co-inhibition of ERK1/2 and ERK5
MAPK pathways**

Christian Adam (ORCID)¹, Lorenza Fusi (ORCID)¹, Neele Weiss (ORCID)¹, Simon G. Goller (ORCID)¹, Katharina Meder (ORCID)¹, Verena G. Frings (ORCID)¹, Hermann Kneitz (ORCID)¹, Matthias Goebeler (ORCID)¹, Roland Houben (ORCID)¹, David Schrama (ORCID)¹, and Marc Schmidt (ORCID)^{1, #}

¹Department of Dermatology, Venereology and Allergology, University Hospital Würzburg, Germany

Running title: ERK5 as target in NRAS-mutant melanoma

[#]Correspondence to: Prof. Dr. Marc Schmidt, Department of Dermatology, Venereology and Allergology, Josef-Schneider-Str. 2, 97080 Würzburg, Germany, Phone: +49-931-201-26396, Fax: +49 931 201 26462, E-mail: schmidt_M11@ukw.de

Word counts:

Abstract: 198

Text: 3994 (without abstract, references, figure legends)

Tables: 1 supplementary table

Figures: 5 main figures, 9 supplementary figures

Abbreviations used: BRAFi, BRAF-V600 inhibitor; EGF, epidermal growth factor receptor; ERK5i, ERK5 inhibitor, KLF, Krüppel-like factor; MEKi, MEK1/2 inhibitor; MAPK, Mitogen-activated protein kinase; MAPKi, RAF/MEK/ERK pathway-directed treatment,

PDGF, platelet-derived growth factor receptor, qPCR, quantitative real time polymerase chain reaction

Journal Pre-proof

ABSTRACT

Cutaneous melanoma is a highly malignant tumor typically driven by somatic mutation in the oncogenes *BRAF* or *NRAS*, leading to uncontrolled activation of the MEK/ERK mitogen-activated protein kinase (MAPK) pathway. Despite the availability of immunotherapy, MAPK-pathway targeting regimens are still a valuable treatment option for BRAF-mutant melanoma. Unfortunately, patients with NRAS mutation do not benefit from such therapies due to the lack of targetable BRAF mutations and a high degree of intrinsic and acquired resistance towards MEK inhibition.

Here we demonstrate that concomitant inhibition of ERK5 removes this constraint and effectively sensitizes NRAS-mutant melanoma cells for MAPK pathway targeting therapy.

Using approved MEK inhibitors or a pharmacological ERK inhibitor, we demonstrate that MAPK inhibition triggers a delayed activation of ERK5 via a PDGFR inhibitor-sensitive pathway in NRAS-mutant melanoma cells resulting in sustained proliferation and survival. ERK5 phosphorylation also occurred naturally in NRAS-mutant melanoma cells and correlated with nuclear localization of its stem cell-associated effector KLF2. Importantly, MEK/ERK5 co-inhibition prevented long-term growth of human NRAS-mutant melanoma cells *in vitro*, and effectively repressed tumor progression in a xenotransplant mouse model.

Our findings suggest MEK/ERK5 co-targeting as potential treatment option for NRAS-mutant melanoma, which currently is not amenable for targeted therapies.

Keywords: ERK5/ Krüppel-like factor/ NRAS/ melanoma/ tumor resistance

INTRODUCTION

Many cancers are characterized by deregulation or oncogene-mediated activation of the growth factor-stimulated RAS/RAF/MEK/ERK Mitogen-activated protein kinase (MAPK) cascade, which promotes proliferation and survival (Samatar and Poulikakos, 2014). Cutaneous melanoma is a prime example since the majority of patients have oncogenic driver mutations in *BRAF* (~50-60 % of patients, e.g. BRAF-V600E) or *NRAS* (~20 % of cases, e.g. NRAS-Q61K/L) (Schadendorf et al., 2015). This fueled the clinical development of small compound inhibitors, including the BRAF-V600 inhibitors (BRAFi) vemurafenib, dabrafenib or encorafenib and the MEK1/2 inhibitors (MEKi) trametinib, cobimetinib and binimetinib. Despite the success of recent immune-oncological approaches, RAF/MEK/ERK pathway-directed treatments (MAPKi) still account for a significant portion of melanoma therapy, especially for advanced BRAF-V600-mutant melanoma (Luke et al., 2017, Ugurel et al., 2017). Unfortunately, development of treatment resistance is a major disadvantage (Luke et al., 2017, Sullivan and Flaherty, 2013). Moreover, patients with NRAS-mutant melanoma do not benefit significantly from MAPKi therapies (Dummer et al., 2017). Partially this is due to oncogene-specificity of the employed BRAFi and mutual exclusivity of oncogenic NRAS and BRAF mutations in untreated melanoma (Schadendorf et al., 2015). Additionally, NRAS-mutant melanomas show a high rate of MEKi resistance that hampers the clinical success of MAPKi therapies (Dummer et al., 2017), leaving only immunotherapy as effective treatment. Yet, immunotherapy can cause serious side effects, and a substantial number of patients exhibit primary resistance to immune-oncological approaches (Luke et al., 2017), underscoring the need for alternative treatments.

One signaling module that recently emerged as therapeutic target for various cancers is the MEK5/ERK5 (BMK1) MAPK pathway (Hoang et al., 2017, Lochhead et al., 2012). Initially described as stress-activated cascade, it is also activated by growth factors in some cell types

(Hayashi and Lee, 2004). Physiologically, ERK5 and its upstream activator MEK5 play essential roles in vascular development/function as well as in endothelial and neuronal survival (Finegan et al., 2009, Hayashi and Lee, 2004, Ohnesorge et al., 2010, Pi et al., 2004). In tumor cells the pathway similarly exerts a cytoprotective function (Carvajal-Vergara et al., 2005, Garaude et al., 2006, Hoang et al., 2017, Pereira et al., 2016), in particular under therapeutic stress. Additionally, ERK5 activation has been implicated with tumor angiogenesis (Hayashi et al., 2005), proliferation (Carvajal-Vergara et al., 2005, Esparis-Ogando et al., 2002, Kato et al., 1998, Mulloy et al., 2003) and tumor plasticity/metastasis (Pavan et al., 2018, Ramsay et al., 2011), albeit controversial data have been published for most of those functions (Hoang et al., 2017, Lochhead et al., 2012).

Recent studies reported that in different RAS tumors ERK5 could also be activated by MEKi treatment thereby contributing to therapy resistance. In KRAS-mutant colon carcinoma cells, trametinib-mediated MEK inhibition triggered a compensatory ERK5 activation via an unknown mechanism allowing proliferation under treatment (de Jong et al., 2016). In KRAS-transformed pancreatic ductal carcinoma, MEKi similarly induced ERK5 activation, which mediated MEKi resistance via cMYC stabilization (Vaseva et al., 2018). The contribution of ERK5 activation to MEKi-resistance of NRAS-mutant melanoma, however, is unclear.

Here we demonstrate that ERK5 signaling is frequently activated in NRAS-mutated melanoma and promotes tumor cell proliferation and survival under MEKi. Trametinib-induced ERK5 phosphorylation was associated with induction of the receptor tyrosine kinase PDGFR β and abrogated by PDGFR inhibition. Xenotransplantation experiments revealed effective suppression of NRAS-driven melanoma by MEKi/ERK5i co-treatment, suggesting MEKi/ERK5i administration as potential treatment strategy for this melanoma subtype.

RESULTS

Pharmacological MEK inhibition results in compensatory ERK5 activation promoting proliferation and survival of NRAS-mutant melanoma cells

The MEK5/ERK5 cascade was recently described as pathway conferring MEKi insensitivity in KRAS-mutant colon carcinoma cells (de Jong et al., 2016). To evaluate whether ERK5 may exert similar functions in NRAS-mutant melanoma, we analyzed ERK5 phosphorylation in 13 different melanoma cell lines previously shown to harbor activating NRAS mutations (Schrama et al., 2008, Ugurel et al., 2007). Intriguingly, immunoblots with an ERK5-specific antiserum detecting both its autophosphorylated and unphosphorylated form (Ohnesorge et al., 2010) revealed prominent ERK5 phosphorylation in ~one third of the cell lines (Fig. 1a). This constitutive ERK5 phosphorylation was required for proliferation as in cell lines with high basal phospho-ERK5 levels, pharmacological ERK5 inhibition using the ERK5 inhibitor XMD8-92 efficiently prevented ERK5 autophosphorylation and S-phase accumulation in combined DNA profiling and BrdU-labelling experiments (Fig. 1b, Fig. S1a, b). Moreover, it reduced total and nuclear protein levels of the ERK5 phosphorylation substrate MEF2C (Fig. S1b,c) that mediates its proliferative responses (Kato et al., 1997). Treatment with increasing concentrations of the MEKi trametinib further enhanced ERK5 phosphorylation in FM79 (Fig. 1c). Additionally, trametinib dose-dependently induced ERK5 phosphorylation in two NRAS Q61-mutated melanoma cell lines (BLM and MaMel26a) and a BRAF-V600E-mutant cell line (LOX-IMVI)(Ikediobi et al., 2006), which lack obvious basal ERK5 autophosphorylation (Fig. 1c). Similar results were obtained with other MEKi (Fig. S2), minimizing the possibility of off-target effects.

ERK5 activation can also promote tumor cell survival, in particular under stress conditions (Hoang et al., 2017, Lochhead et al., 2012). To study if ERK5 activation might allow NRAS-

mutant melanoma cells to escape MEKi-induced cell death, we treated FM79 cells with trametinib +/- XMD8-92, and quantified the percentage of dead cells 72h later by 7-AAD/Annexin V co-staining. XMD8-92 monotreatment failed to induce cytotoxicity in absence of MEKi (Fig. 1d and Fig. S3a), but dramatically increased trametinib-induced cytotoxicity. Similarly, combination of trametinib with siRNA for ERK5 (Fig. 1e, Fig. S3b) or MEK5 (Fig. S3c) resulted in enhanced cytotoxicity, confirming that MEK5/ERK5 inhibition was responsible. A synergistic apoptotic response was also evident by immunoblots for cleaved Caspase 3 (Fig. 1f). Additionally, crystal violet assays confirmed an improved antiproliferative/cytotoxic effect in all cell lines tested (Fig. 1g, Fig. S4a, b). We could also reproduce these data by using cobimetinib as an alternative MEKi (Fig. S4c), replacement of XMD8-92 by the MEK5 inhibitor BIX02188 (Fig. S4d), or combination of trametinib with stable small hairpin-mediated ERK5 depletion (Fig. S4e).

ERK5 inhibition improves long-term sensitivity to MEKi

To explore if XMD8-92 co-treatment may also prevent long-term MEKi resistance we treated BLM with low doses of trametinib or XMD8-92 alone, or in combination for a period of four weeks, and investigated the effects on proliferation/survival by cell doubling time analysis. While trametinib- and XMD8-92-treated cells exhibited slightly higher doubling times, cell numbers still increased over time and cells had to be split repeatedly (Fig. 2a). In contrast, combined XMD8-92/trametinib treatment strongly suppressed tumor cell proliferation as evident by a substantially increased doubling time (Fig. 2a). Unlike all other conditions, the co-treated cells also did not require splitting during the whole observation period. Similar results were obtained when long-term proliferation of BLM was analyzed by labelling with the live cell dyes CFSE or DDAO-SE: Both XMD-8-92 co-treatment (Fig. 2b) and stable ERK5 knockdown (Fig. 2c) dramatically enhanced the antiproliferative effect of trametinib as indicated by dye retention. By contrast, neither drug monotreatment nor ERK5 depletion

alone had a permanent impact on proliferation. A similar sustained growth arrest was observed upon XMD8-92/trametinib co-incubation of FM79 (Fig. 2d), MaMel26a and the BRAF-mutant LOX-IMVI cell line (Fig. S5a). For those cell lines, we further observed a strong loss of cells upon trametinib/XMD8-92 co-incubation (Fig. S5b), suggesting that MEKi/ERK5i co-treatment improves long-term drug effectiveness. However, all test cell lines retained their ability to initiate proliferation as cell numbers recovered when inhibitors were removed after 2-4 weeks of treatment (Fig. 2e, Fig. S5a).

ERK5 phosphorylation is a delayed response to ERK1/2 inhibition and is associated with PDGFR β induction

We next investigated if ERK5 phosphorylation was dependent on the MEK target ERK1/2. Pharmacological inhibition using the ERK1/2 inhibitor GDC-0994 impaired growth of BLM in crystal violet assays at concentrations ≥ 5 -10 μ M (Fig. S6a). At those effective doses, we observed a concentration-dependent ERK5 phosphorylation (Fig. S6b), loss of mRNA expression of the ERK1/2 target gene *DUSP4* (Cagnol and Rivard, 2013) (Fig. S6c), and a synergistic decrease of melanoma cell survival upon XMD8-92 co-treatment (Fig. 3a, Fig. S6d). This validates that loss of ERK1/2 activity was sufficient to trigger ERK5 activation and that ERK5 inhibition can also augment ERK inhibitor-induced cytotoxicity.

Interestingly, comparison of the kinetics of GDC-0994- and trametinib-induced ERK5 phosphorylation in BLM disclosed that ERK5 phosphorylation increased ~ 8 -16 h after drug administration whereas *DUSP4* mRNA/protein expression and ERK1/2 phosphorylation diminished as early as 2 h after GDC-0994 or trametinib treatment (Fig. 3b, c). Accordingly, ERK5 activation is an indirect consequence of ERK1/2 inhibition.

An important resistance mechanism of MAPKi in BRAF-mutant melanoma cells is the upregulation of tyrosine kinase signaling (Girotti et al., 2013, Nazarian et al., 2010, Sun et al.,

2014). This includes activation of the epidermal growth factor receptor (EGFR) family that can activate ERK5 in some cell types (Kato et al., 1998, Yang et al., 2010). However, co-incubation with different pan-EGFR inhibitors failed to suppress trametinib-induced ERK5 phosphorylation in BLM (Fig. 3d) albeit inhibitors and EGF signaling were functional as they abolished EGF-induced ERK5 activation at the highest drug concentration (Fig. S7a, b). Similarly, pharmacological inhibition of insulin growth factor 1 receptor that was reported to mediate MAPKi-induced ERK5 activation in BRAF-mutant melanoma (Benito-Jardon et al., 2019), did not affect trametinib-dependent ERK5 phosphorylation in BLM (Fig. S7c). Instead, pan-blockade of platelet-derived growth factor receptor (PDGFR) signaling, which has been implicated with BRAFi resistance in melanoma (Nazarian et al., 2010) and could stimulate ERK5 in some cells (Izawa et al., 2007, Lennartsson et al., 2010, Rovida et al., 2008), dose-dependently inhibited trametinib-induced ERK5 phosphorylation in BLM (Fig. 3e), MaMel26a and the BRAF-mutant LOX-IMVI cell line (Fig. S8a). We also observed strongly increased surface expression of PDGFR β but not PDGFR α upon MEKi in those cell lines with low basal phospho-ERK5 levels (Fig. 3f, Fig. S8b,c). In FM79, which show constitutive ERK5 phosphorylation, trametinib treatment did not induce detectable PDGFR β protein expression but similarly to BLM enhanced *PDGFRB* mRNA expression (Fig. S8b, c). PDGFR inhibition did not suppress basal ERK5 phosphorylation in FM79 but prevented the trametinib-induced increase of ERK5 phosphorylation (Fig. S8a). Thus, PDGFR signaling appears to be important for MEKi-induced ERK5 phosphorylation but dispensable for the constitutive ERK5 phosphorylation in the melanoma cell lines tested.

ERK5 phosphorylation triggers KLF2 expression and nuclear localization in NRAS-mutant melanoma

Key transcriptional ERK5 effectors in other cell types are the Krüppel-like transcription factors KLF2 and KLF4 (Ohnesorge et al., 2010, Sohn et al., 2005). KLF4 can act as context-

specific oncogene that overcomes RAS-induced senescence (Rowland et al., 2005). Moreover, both KLFs are involved in the regulation of stem cell-like properties (Wernig et al., 2007, Yeo et al., 2014), which may promote tumor resistance. Quantitative real time polymerase chain reaction (qPCR) analysis revealed a robust and significant induction of *KLF2* mRNA by trametinib in both BLM and FM79 that was sensitive to ERK5 inhibition (Fig. S9a and b). By contrast, *KLF4* induction was somewhat variable and did not reach statistical significance. However, in cell lines, with enhanced basal pERK5 levels (FM79 or M26) XMD8-92 treatment or MEK5 knockdown significantly reduced basal expression of both genes (Fig. S9b-d) confirming *KLF4* as additional ERK5 target in NRAS-mutant melanoma cells. Importantly, immunofluorescence staining revealed a distinct nuclear staining pattern of KLF2 in both untreated FM79 and trametinib-treated BLM or FM79. By contrast, KLF2 staining was largely cytoplasmic in untreated BLM or when the cell lines were exposed to XMD8-92 +/- trametinib (Fig. 4a, b). Thus, ERK5 activation not only increases transcription but also activity of KLF2 by promoting its nuclear localization.

Immunohistochemical analysis of KLF2 in 18 tumor samples of patients with validated NRAS Q61-mutant primary or metastatic melanoma confirmed nuclear KLF2 staining in ~30% of the totally investigated samples (5/12 metastatic and 1/6 primary melanomas) (Table S1). Patterns were usually heterogeneous and appeared to be locally restricted to the tumor edge or limited to single tumor cells within the melanoma tissue (Fig. 4c). Nevertheless, these data suggest that ERK5 activation and subsequent KLF2 relocalization to the nucleus also occur naturally in human NRAS-driven melanoma.

MEKi/ERK5i co-treatment suppresses tumor growth of NRAS-mutant melanoma *in vivo*

We finally performed xenotransplantation experiments with BLM or FM79 melanoma cells in immune-deficient NOD/SCID mice. In agreement with our *in vitro* experiments, trametinib monotherapy initially delayed tumor growth of xenotransplanted BLM compared to vehicle-treatment but ultimately failed to suppress tumor expansion. By contrast, XMD8-92 monotherapy did not affect volume increase of BLM-derived melanoma over time but strongly suppressed tumor growth when co-administered with trametinib (Fig. 5a). Visual inspection at the experimental endpoint revealed consistently smaller tumors sizes for the trametinib/XMD8-92 cohort in comparison to all other treatments (Fig. 5b). Similarly, XMD8-92/trametinib co-treatment dramatically suppressed tumor growth of xenotransplanted FM79 melanoma cells (Fig. 5c, d). However, in line with the high basal ERK5 activity, we observed a transient inhibitory effect by XMD8-92 mono-treatment on FM79 xenotransplants. Moreover, trametinib monotherapy was somewhat less effective (Fig. 5c). Thus, ERK5 activity in the FM79 cell line may confer some intrinsic MEKi resistance and proliferation advantage that may be transient and subject to plasticity. Nevertheless, with both cell lines we failed to observe any tumor volume increase for the XMD8-92/trametinib-treated group, suggesting that the drug co-administration may completely suppress growth of NRAS-mutant melanoma and counteract resistance development.

Finally, we analyzed KLF2 expression as marker for ERK5 activity. Immunostaining of tumor tissue from BLM- or FM79-derived tumors revealed an increased staining intensity and a more pronounced nuclear localization upon trametinib treatment, which were largely lost under XMD8-92 co-administration (Fig. 5e). Vehicle-treated FM79 tumors showed a distinct nuclear pattern, which shifted to a more faint and cytoplasmic localization upon XMD8-92 treatment. For the BLM-derived control tumors, KLF2 staining was less intense and more

variable with a higher degree of cytoplasmic staining (Fig. 5e). Consistent with our *in vitro* experiments this suggests that basal ERK5 activity is unlikely to be an absolute requirement for expansion of NRAS-mutant tumors but may provide a proliferation/survival advantage, especially under treatment.

DISCUSSION

Here we analyzed whether the ERK5 MAPK pathway might contribute to MEKi resistance in human NRAS-driven melanoma cells. Both our *in vitro* and xenotransplantation experiments support this view and provide evidence that concomitant inhibition of MEK and ERK5 could be an efficient way to treat NRAS-driven advanced melanoma.

ERK5 activation was previously found to compensate MEKi-induced tumor suppression in different KRAS-transformed tumor cells (de Jong et al., 2016, Vaseva et al., 2018). Additionally, several current studies reported that in BRAF-V600-mutant melanoma cells MAPKi by BRAFi/ERKi monotherapy or BRAFi/MEKi combination treatment could also induce ERK5 activity thereby preventing therapy resistance (Benito-Jardon et al., 2019, Song et al., 2017, Tusa et al., 2018). Our experiments with the BRAF-mutant LOX-IMVI cell line expand these data to MEKi monotreatment. Hence, ERK5 activation may play a broader role as MEKi resistance pathway. Of note, the mechanisms of MAPKi-induced ERK5 activation might vary between different tumors, oncogenes and cell lines. In KRAS-transformed pancreatic ductal carcinoma, for instance, MEKi-induced ERK5 activation required EGFR activation (Vaseva et al., 2018). By contrast, neither in our experiments nor in KRAS-mutant colon carcinoma (de Jong et al., 2016) a critical contribution of EGFR for trametinib-dependent ERK5 activation was found. Our data also argue against an involvement of the insulin-like growth factor 1 receptor, which mediated ERK inhibitor-induced ERK5 phosphorylation in the BRAF-V600-mutant melanoma cell line A375 (Benito-Jardon et al.,

2019). Instead, in NRAS-mutant melanoma increased PDGFR β signaling could be responsible. Enhanced PDGFR β signaling was previously implicated with BRAFi resistance in BRAF-V600-mutant melanoma cells (Nazarian et al., 2010), but its consequence for ERK5 activation was not analyzed. Our data show that trametinib-induced ERK5 phosphorylation in the BRAF-mutant LOX-IMVI cell line at least was sensitive to PDGFR inhibition. Regardless whether PDGFR β signaling is more frequently involved in MAPKi-induced ERK5 activation or if oncogene/cell line-specific differences or redundancies exist (as indicated by our failure to inhibit basal ERK5 phosphorylation in FM79), our results suggest that ERK5 activation may be a common route of melanoma cells to escape MEKi-induced tumor suppression. This implies that that even a large group of melanoma patients might benefit from MEKi/ERK5i-based therapy.

An intriguing observation was the occurrence of basal ERK5 activity in different NRAS-mutant melanoma cells. Our examination of the ERK5-activated FM79 cell line clearly shows that ERK5 phosphorylation provides a proliferation advantage to those cells, although earlier studies with other RAS-mutant tumor cell types demonstrated that certainly not all of them depend on ERK5 activity for proliferation (Lochhead et al., 2016). Surprisingly, ERK5 activity was not required for survival in any of our tested cell lines unless additionally MEK1/2 or ERK1/2 were inhibited. The latter finding is in conflict with previous results from *MEK5* and *ERK5* knockout mouse models (Hayashi et al., 2004, Wang et al., 2005) and subsequent studies with several primary cell types including endothelial cells (Ohnesorge et al., 2010, Pi et al., 2004) and neuronal cells (Finegan et al., 2009), where the MEK5/ERK5 cascade plays a critical role as survival pathway. Notably, we did not observe overt neuronal or vascular defects in our XMD8-92 mono-treated or XMD8-92/trametinib co-treated mice. Albeit the reason for this discrepancy is unclear, our results are consistent with previous reports that employed XMD8-92 *in vivo* (de Jong et al., 2016, Tusa et al., 2018, Vaseva et al.,

2018, Yang et al., 2010). It is conceivable that ERK5 activity may not be a *bona fide* survival signal but only promotes survival under certain conditions such as cellular stress. Consistently, in KRAS-mutant colon carcinoma cells ERK5 activity conferred chemoresistance to 5-fluorouracil, but did not affect survival in absence of 5-fluorouracil (Pereira et al., 2016). It is tempting to speculate that particularly an enhanced stress resistance and not a generally enhanced survival or proliferation may account for the high rate of ERK5 activation in NRAS-mutant melanoma. This is also corroborated by the fact that XMD8-92 monotreatment effectively inhibited proliferation of FM79 cells in short-term assays *in vitro*, but only mildly impaired long-term tumor growth in in our CFSE experiments and our xenotransplantation model.

Another discovery requiring further examination is our finding that ERK5 activity was associated with nuclear localization of KLF2. Many groups including our own have established ERK5 as essential regulator of *KLF2* transcription (Ohnesorge et al., 2010, Sohn et al., 2005). Additionally, we now show regulation of KLF2 localization by ERK5. Especially the KLF2 staining pattern of our xenotransplanted tumor cells, which correlated well with the expected outcome of the applied inhibitors, suggests that KLF2 nuclear localization reliably reflects the ERK5 phosphorylation status of the respective tumor cells. Nevertheless, at this stage we cannot exclude that the observed KLF2 localization in human melanoma may also be regulated by yet unknown signals. Unfortunately, the current lack of specific ERK5 antibodies suitable for immunostaining together with an observed cross-reactivity of different commercially available phospho-ERK5 antibodies with phospho-ERK1/2 in immunoblots (own unpublished observations) precluded a direct *in situ* analysis of ERK5 activation in melanoma samples. The more important question, however, concerns the functional consequence of the observed nuclear localization of KLF2 in NRAS-mutant melanoma, which is currently unclear. Future studies should address this important issue.

In summary, our data imply that MEKi/ERK5i co-treatment could improve the effectiveness of available MEKi therapies in patients suffering from NRAS-mutated melanoma and might provide a therapeutic avenue for patients not eligible or resistant to immunotherapeutic approaches.

MATERIALS AND METHODS

Ethics statement

The presented work was conducted in accordance with the Declaration of Helsinki. The generation and characterization of melanoma patient material was approved by the Institutional Review Board of the University Hospital Würzburg (study numbers 169/12 and 241/14). Written informed consent was obtained from all patients. Animal experiments were performed according the NIH Guide for the Care and Use of Laboratory Animals and approved by the local authorities (Government of Unterfranken; animal experiment application 55.2.2-2532-2-619-15).

Cell culture and reagents

All human melanoma cell lines have previously been characterized regarding their *NRAS* and *BRAF* mutation status (Ikediobi et al., 2006, Schrama et al., 2008, Ugurel et al., 2007) and were recovered freshly from the frozen stock collection of the Department of Dermatology, Würzburg. Cells were grown at 37°C/5% CO₂ in RPMI1640 Glutamax (ThermoFisher, Darmstadt, Germany) supplemented with 10% fetal bovine serum (Merck, Darmstadt, Germany) for maximally 20 passages. BLM and FM79 were routinely tested for mycoplasma negativity using a commercial PCR-based detection kit (Applichem, Darmstadt, Germany) and their identity confirmed by commercial short tandem repeats analysis (Microsynth AG, Balgach, Switzerland; last test: October 2019). BLM single cell clones stably expressing

small-hairpin RNA against *ERK5* (Ohnesorge et al., 2010) were generated and tested as detailed in the supplementary information.

Trametinib was obtained from Enzo, Lörrach, Germany, and used at 100 nM, unless indicated otherwise. Small quantities of the ERK5 inhibitor XMD8-92 for *in vitro* experiments were purchased from Santa Cruz, Heidelberg, Germany, and routinely employed at 10 μ M; greater quantities used for the xenotransplantation experiments were from Axon Medchem, Groningen, Netherlands. All other pharmacological inhibitors were purchased from Selleckchem, Munich, Germany. Recombinant human EGF (#AF-100-15) was from Peptidech, Hamburg, Germany.

Antibodies and immunoblot

Melanoma cells were lysed and protein expression analyzed by immunoblot as described (Ohnesorge et al., 2010) using the following primary antibodies: phospho-ERK1/2 (#9101), MEF2C (#5030), DUSP4 (#5149), Cell signaling, Frankfurt, Germany; ERK5 (#E1523), α -tubulin (#T5168), Sigma-Aldrich, Darmstadt, Germany.

siRNA transfection

siRNA transfections were performed using Lipofectamine® RNAiMAX (ThermoFisher, Darmstadt, Germany) following the manufacturer's guidelines. Details are given as supplementary information.

RNA isolation and qPCR

Total cellular RNA was isolated and reversely transcribed into cDNA employing commercially available kits from Qiagen, Hilden, Germany, according to the manufacturer's instructions. Relative mRNA expression of the respective genes was determined by TaqMan-based qPCR using commercially available probes (*GAPDH*: hs99999905_m1, *KLF2*:

hs00360439_g1, *KLF4*: hs00358836_m1) and appropriate chemistry from ThermoFisher, Darmstadt, Germany. Alternatively, SYBR-Green-based qPCR detection with gene-specific primer pairs (sequences available upon request) and an appropriate qPCR kit (ThermoFisher, Darmstadt, Germany) was used. Test gene expression was each normalized to expression of *GAPDH* and related to an experimental control using the comparative threshold cycle method.

Analysis of proliferation and viability

Short-term cell viability and proliferation was monitored by crystal violet staining of attached live cells, 7AAD/Annexin V staining, or 5-bromo-2'-deoxyuridine (BrdU) labelling as detailed in the supplementary information.

Long-term proliferation of the differently treated cells was studied by cell doubling time analysis over a period of 4 weeks. Alternatively, cells were labelled with the cell-activated fluorescent live dyes CFSE (carboxyfluorescein diacetate succinimidyl ester) or DDAO-SE (decyl dimethyl amine oxide succinimidyl ester) (ThermoFisher, Darmstadt, Germany) and relative fluorescence intensity losses upon treatment analyzed by flow cytometry. Details are provided as supplementary information.

PDGFR surface staining

The different PDGFR isoforms were stained using directly fluorescent-coupled antibodies against PDGFR α (#130-115-337) or PDGFR β (#130-121-128, Miltenyi Biotec, Bergisch Gladbach, Germany) according to the manufacturer's protocol and surface expression analyzed by flow cytometry. Isotype-specific control staining served as background reference.

Immunofluorescence and immunohistochemistry

To determine KLF2 protein expression and localization, cells grown on coverslips, formalin-fixed and paraffin-embedded (FFPE) tumor tissue from patients with NRAS Q61L/R-positive

primary or metastatic melanoma (validated by panel sequencing), or FFPE samples from xenografted tumors were stained using an affinity-purified rabbit antiserum against human KLF2 (#HPA055964, Sigma-Aldrich, Darmstadt, Germany) as detailed in the supplementary information.

Xenograft model, tumor induction and treatment protocols

Female NOD.CB17-Prkdc^{Scid}/J (NOD/SCID) mice were obtained from Charles River Laboratories, Sulzfeld, Germany, at the age of eight weeks. Mice were housed under pathogen-free conditions according to the animal care guidelines of the University Hospital Würzburg. Tumors were established by subcutaneous injection of 5×10^5 BLM or FM79 cells (mixed 1:2 with MatriGel, BD Biosciences; Heidelberg, Germany) in 100 μ l final volume into the lateral flank. The tumor volume (V) was determined by daily diameter measurement in two dimensions with a slide gauge according to the formula: $V = \pi/6 \times a^2 \times b$ (*a*: length; *b*: width). Once tumors reached a volume of ~ 150 mm³, mice were randomized into four groups of 5 (controls) or 6-7 (treatment) mice. Mice were treated by daily successive intraperitoneal injections of 100 mg/kg XMD8-92 in 30% 2-hydroxypropyl- β -cyclodextrin, 100 μ g/kg trametinib in PBS/1% DMSO, or the respective vehicles for 14 days, and sacrificed at day 15 for collection, formalin-fixation and paraffin-embedding of the tumors.

DATA AVAILABILITY STATEMENT

No datasets were generated or analyzed during the current study.

CONFLICT OF INTEREST

The authors declare no conflict of interests.

ACKNOWLEDGEMENTS

We thank Svenja Meierjohann and Bastian Schilling for helpful discussion and suggestions, and Helga Sennefelder for excellent technical assistance. This work was funded by grants from the *Deutsche Forschungsgemeinschaft* (DFG; grants DFG SCHM2460/3-1 and DFG SCHM2460/2-1 to M.S.).

Author contributions

Conceptualization: MS., DS, RH; Formal analysis: CA, LF, NW, SGG, VGF, HK; Funding acquisition: MS; Investigation: CA, LF; NW, SGG, KM; MS; Methodology: CA, MS; Project Administration: MS; Resources: MG; Supervision: MS; Validation: NW, SGG, MS; Visualization: CA, MS; Writing: MS, CA; Writing- Review and Editing: MS, DS, RH, MG.

REFERENCES

- Benito-Jardon L, Diaz-Martinez M, Arellano-Sanchez N, Vaquero-Morales P, Esparis-Ogando A, Teixido J. Resistance to MAPK Inhibitors in Melanoma Involves Activation of the IGF1R-MEK5-Erk5 Pathway. *Cancer Res* 2019;79:2244-56.
- Cagnol S, Rivard N. Oncogenic KRAS and BRAF activation of the MEK/ERK signaling pathway promotes expression of dual-specificity phosphatase 4 (DUSP4/MKP2) resulting in nuclear ERK1/2 inhibition. *Oncogene* 2013;32:564-76.
- Carvajal-Vergara X, Tabera S, Montero JC, Esparis-Ogando A, Lopez-Perez R, Mateo G, et al. Multifunctional role of Erk5 in multiple myeloma. *Blood* 2005;105:4492-9.
- de Jong PR, Taniguchi K, Harris AR, Bertin S, Takahashi N, Duong J, et al. ERK5 signalling rescues intestinal epithelial turnover and tumour cell proliferation upon ERK1/2 abrogation. *Nat Commun* 2016;7:11551.
- Dummer R, Schadendorf D, Ascierto PA, Arance A, Dutriaux C, Di Giacomo AM, et al. Binimetinib versus dacarbazine in patients with advanced NRAS-mutant melanoma (NEMO): a multicentre, open-label, randomised, phase 3 trial. *Lancet Oncol* 2017;18:435-45.
- Esparis-Ogando A, Diaz-Rodriguez E, Montero JC, Yuste L, Crespo P, Pandiella A. Erk5 participates in neuregulin signal transduction and is constitutively active in breast cancer cells overexpressing ErbB2. *Mol Cell Biol* 2002;22:270-85.
- Finegan KG, Wang X, Lee EJ, Robinson AC, Tournier C. Regulation of neuronal survival by the extracellular signal-regulated protein kinase 5. *Cell Death Differ* 2009;16:674-83.
- Garaude J, Cherni S, Kaminski S, Delepine E, Chable-Bessia C, Benkirane M, et al. ERK5 activates NF-kappaB in leukemic T cells and is essential for their growth in vivo. *J Immunol* 2006;177:7607-17.
- Girotti MR, Pedersen M, Sanchez-Laorden B, Viros A, Turajlic S, Niculescu-Duvaz D, et al. Inhibiting EGF receptor or SRC family kinase signaling overcomes BRAF inhibitor resistance in melanoma. *Cancer Discov* 2013;3:158-67.
- Hayashi M, Fearn C, Eliceiri B, Yang Y, Lee JD. Big mitogen-activated protein kinase 1/extracellular signal-regulated kinase 5 signaling pathway is essential for tumor-associated angiogenesis. *Cancer Res* 2005;65:7699-706.
- Hayashi M, Kim SW, Imanaka-Yoshida K, Yoshida T, Abel ED, Eliceiri B, et al. Targeted deletion of BMK1/ERK5 in adult mice perturbs vascular integrity and leads to endothelial failure. *J Clin Invest* 2004;113:1138-48.
- Hayashi M, Lee JD. Role of the BMK1/ERK5 signaling pathway: lessons from knockout mice. *J Mol Med (Berl)* 2004;82:800-8.
- Hoang VT, Yan TJ, Cavanaugh JE, Flaherty PT, Beckman BS, Burow ME. Oncogenic signaling of MEK5-ERK5. *Cancer Lett* 2017;392:51-9.
- Ikedobi ON, Davies H, Bignell G, Edkins S, Stevens C, O'Meara S, et al. Mutation analysis of 24 known cancer genes in the NCI-60 cell line set. *Mol Cancer Ther* 2006;5:2606-12.
- Izawa Y, Yoshizumi M, Ishizawa K, Fujita Y, Kondo S, Kagami S, et al. Big mitogen-activated protein kinase 1 (BMK1)/extracellular signal regulated kinase 5 (ERK5) is involved in

- platelet-derived growth factor (PDGF)-induced vascular smooth muscle cell migration. *Hypertens Res* 2007;30:1107-17.
- Kato Y, Kravchenko VV, Tapping RI, Han J, Ulevitch RJ, Lee JD. BMK1/ERK5 regulates serum-induced early gene expression through transcription factor MEF2C. *EMBO J* 1997;16:7054-66.
- Kato Y, Tapping RI, Huang S, Watson MH, Ulevitch RJ, Lee JD. Bmk1/Erk5 is required for cell proliferation induced by epidermal growth factor. *Nature* 1998;395:713-6.
- Lennartsson J, Burovic F, Witek B, Jurek A, Heldin CH. Erk 5 is necessary for sustained PDGF-induced Akt phosphorylation and inhibition of apoptosis. *Cell Signal* 2010;22:955-60.
- Lochhead PA, Clark J, Wang LZ, Gilmour L, Squires M, Gilley R, et al. Tumor cells with KRAS or BRAF mutations or ERK5/MAPK7 amplification are not addicted to ERK5 activity for cell proliferation. *Cell Cycle* 2016;15:506-18.
- Lochhead PA, Gilley R, Cook SJ. ERK5 and its role in tumour development. *Biochem Soc Trans* 2012;40:251-6.
- Luke JJ, Flaherty KT, Ribas A, Long GV. Targeted agents and immunotherapies: optimizing outcomes in melanoma. *Nat Rev Clin Oncol* 2017;14:463-82.
- Mulloy R, Salinas S, Philips A, Hipskind RA. Activation of cyclin D1 expression by the ERK5 cascade. *Oncogene* 2003;22:5387-98.
- Nazarian R, Shi H, Wang Q, Kong X, Koya RC, Lee H, et al. Melanomas acquire resistance to B-RAF(V600E) inhibition by RTK or N-RAS upregulation. *Nature* 2010;468:973-7.
- Ohnesorge N, Viemann D, Schmidt N, Czymai T, Spiering D, Schmolke M, et al. Erk5 activation elicits a vasoprotective endothelial phenotype via induction of Kruppel-like factor 4 (KLF4). *J Biol Chem* 2010;285:26199-210.
- Pavan S, Meyer-Schaller N, Diepenbruck M, Kalathur RKR, Saxena M, Christofori G. A kinome-wide high-content siRNA screen identifies MEK5-ERK5 signaling as critical for breast cancer cell EMT and metastasis. *Oncogene* 2018;37:4197-213.
- Pereira DM, Simoes AE, Gomes SE, Castro RE, Carvalho T, Rodrigues CM, et al. MEK5/ERK5 signaling inhibition increases colon cancer cell sensitivity to 5-fluorouracil through a p53-dependent mechanism. *Oncotarget* 2016;7:34322-40.
- Pi X, Yan C, Berk BC. Big mitogen-activated protein kinase (BMK1)/ERK5 protects endothelial cells from apoptosis. *Circ Res* 2004;94:362-9.
- Ramsay AK, McCracken SR, Soofi M, Fleming J, Yu AX, Ahmad I, et al. ERK5 signalling in prostate cancer promotes an invasive phenotype. *Br J Cancer* 2011;104:664-72.
- Rovida E, Navari N, Caligiuri A, Dello Sbarba P, Marra F. ERK5 differentially regulates PDGF-induced proliferation and migration of hepatic stellate cells. *J Hepatol* 2008;48:107-15.
- Rowland BD, Bernards R, Peeper DS. The KLF4 tumour suppressor is a transcriptional repressor of p53 that acts as a context-dependent oncogene. *Nat Cell Biol* 2005;7:1074-82.
- Samatar AA, Poulikakos PI. Targeting RAS-ERK signalling in cancer: promises and challenges. *Nat Rev Drug Discov* 2014;13:928-42.

- Schadendorf D, Fisher DE, Garbe C, Gershenwald JE, Grob JJ, Halpern A, et al. Melanoma. *Nat Rev Dis Primers* 2015;1:15003.
- Schrama D, Keller G, Houben R, Ziegler CG, Vetter-Kauczok CS, Ugurel S, et al. BRAFV600E mutations in malignant melanoma are associated with increased expressions of BAALC. *J Carcinog* 2008;7:1.
- Sohn SJ, Li D, Lee LK, Winoto A. Transcriptional regulation of tissue-specific genes by the ERK5 mitogen-activated protein kinase. *Mol Cell Biol* 2005;25:8553-66.
- Song C, Wang L, Xu Q, Wang K, Xie D, Yu Z, et al. Targeting BMK1 Impairs the Drug Resistance to Combined Inhibition of BRAF and MEK1/2 in Melanoma. *Sci Rep* 2017;7:46244.
- Sullivan RJ, Flaherty K. MAP kinase signaling and inhibition in melanoma. *Oncogene* 2013;32:2373-9.
- Sun C, Wang L, Huang S, Heynen GJ, Prahallad A, Robert C, et al. Reversible and adaptive resistance to BRAF(V600E) inhibition in melanoma. *Nature* 2014;508:118-22.
- Tusa I, Gagliardi S, Tubita A, Pandolfi S, Urso C, Borgognoni L, et al. ERK5 is activated by oncogenic BRAF and promotes melanoma growth. *Oncogene* 2018;37:2601-14.
- Ugurel S, Rohmel J, Ascierto PA, Flaherty KT, Grob JJ, Hauschild A, et al. Survival of patients with advanced metastatic melanoma: the impact of novel therapies-update 2017. *Eur J Cancer* 2017;83:247-57.
- Ugurel S, Thirumaran RK, Bloethner S, Gast A, Sucker A, Mueller-Berghaus J, et al. B-RAF and N-RAS mutations are preserved during short time in vitro propagation and differentially impact prognosis. *PLoS One* 2007;2:e236.
- Vaseva AV, Blake DR, Gilbert TSK, Ng S, Hostetter G, Azam SH, et al. KRAS Suppression-Induced Degradation of MYC Is Antagonized by a MEK5-ERK5 Compensatory Mechanism. *Cancer Cell* 2018;34:807-22 e7.
- Wang X, Merritt AJ, Seyfried J, Guo C, Papadakis ES, Finegan KG, et al. Targeted deletion of mek5 causes early embryonic death and defects in the extracellular signal-regulated kinase 5/myocyte enhancer factor 2 cell survival pathway. *Mol Cell Biol* 2005;25:336-45.
- Wernig M, Meissner A, Foreman R, Brambrink T, Ku M, Hochedlinger K, et al. In vitro reprogramming of fibroblasts into a pluripotent ES-cell-like state. *Nature* 2007;448:318-24.
- Yang Q, Deng X, Lu B, Cameron M, Fearn C, Patricelli MP, et al. Pharmacological inhibition of BMK1 suppresses tumor growth through promyelocytic leukemia protein. *Cancer Cell* 2010;18:258-67.
- Yeo JC, Jiang J, Tan ZY, Yim GR, Ng JH, Goke J, et al. Klf2 is an essential factor that sustains ground state pluripotency. *Cell Stem Cell* 2014;14:864-72.

FIGURE LEGENDS

Figure 1. ERK5 activation in NRAS-mutant melanoma cells. (a) Immunoblot showing ERK5 and ERK1/2 phosphorylation in 13 NRAS-mutant human melanoma lines. (b) Analysis of DNA content/BrdU incorporation and ERK5 phosphorylation 48h after treatment of FM79 +/- 10 μ M XMD8-92. (c) ERK5 phosphorylation 48h after increasing trametinib incubation of the specified cell lines. (d, e) Mean (n=3) percentile cytotoxicity \pm s.d. of untransfected (d) or scrambled (siScr)/siERK5-transfected FM79 as quantified by flow analysis of annexin V/7-AAD positivity 72h after the indicated treatments (trametinib: 5 nM, XMD8-92: 10 μ M) (f) Caspase 3 cleavage (Caspase 3* p17/p19) and ERK5 phosphorylation in the specified cell lines 48h after the respective treatments (XMD8-92: 5 μ M, trametinib: 5-25 nM). (g) Crystal violet staining and corresponding immunoblots of BLM treated as specified.

Figure 2. ERK5 inhibition improves long-term MEKi sensitivity of NRAS-mutant melanoma cells. (a) Cell doubling analysis of BLM cultured in growth medium (vehicle), or medium containing the indicated inhibitors for 4 weeks. Individual dots represent doubling times between subsequent passages with numbers denoting passages until the experimental endpoint. (b-d) Representative (n=3) analysis of drug-induced proliferation arrest by quantification of fluorescence intensity retention of CFSE or DDAO-SE live-dye-labeled BLM (b), BLM single clones expressing ERK5 small-hairpin RNA (pRS-ERK5) or empty vector (pRS) (c), or FM79 after two-week treatment with the specified drugs. (d) Crystal violet staining of BLM reseeded 28 days after trametinib/XMD8-92 treatment and incubated with (continuous) or without inhibitors (released) for 5 days. Drug concentrations: 25nM trametinib/2.5 μ M XMD8-92 (BLM); 5nM trametinib/10 μ M XMD8-92 (FM79).

Figure 3. MEKi-induced ERK5 phosphorylation is a delayed response to ERK1/2 inhibition and sensitive to PDGFR inhibition. (a) Synergistic cytotoxicity of BLM by

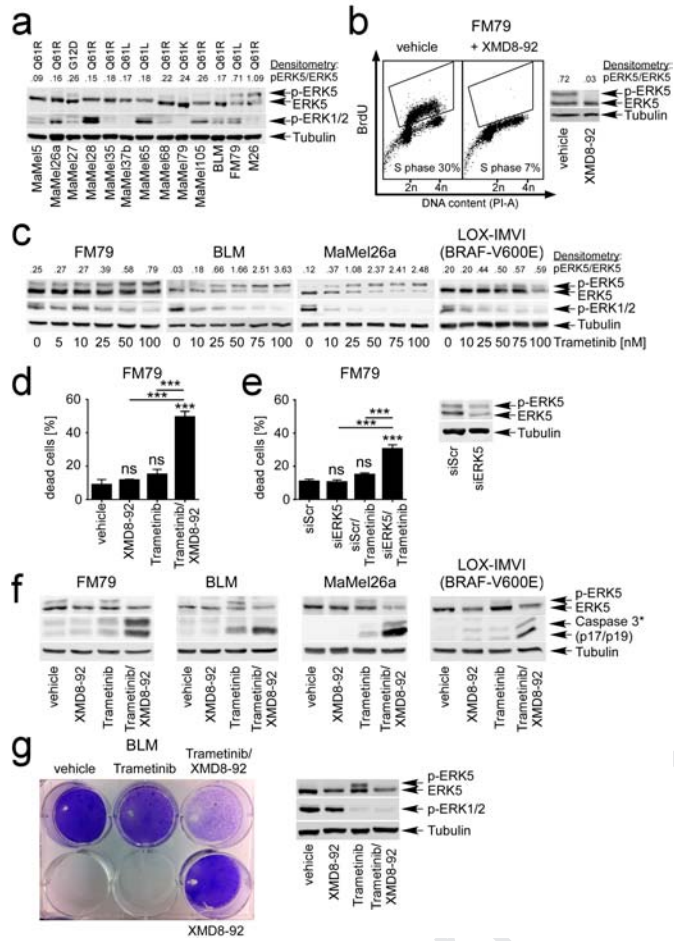
GDC-0994/XMD8-92 (5 μ M, 72h each) co-treatment as visualized by crystal violet staining. (b) Kinetics of *DUSP4* mRNA suppression and ERK5 protein phosphorylation in BLM exposed to GDC-0994. Depicted is the mean (n=3) *GAPDH*-normalized *DUSP4* expression \pm s.d. along with a representative ERK5 immunoblot. (c) Immunoblot, showing trametinib-mediated ERK5 phosphorylation in relation to *DUSP4* protein loss in BLM. (d, e) BLM were treated for 48h with trametinib +/- the indicated pan-EGFR (d) or pan-PDGFR inhibitors (e) at the indicated doses and analyzed for ERK5 phosphorylation by immunoblot. (f) Flow-mediated quantification of PDGFR α and β surface expression in untreated or 48h trametinib-treated BLM cells.

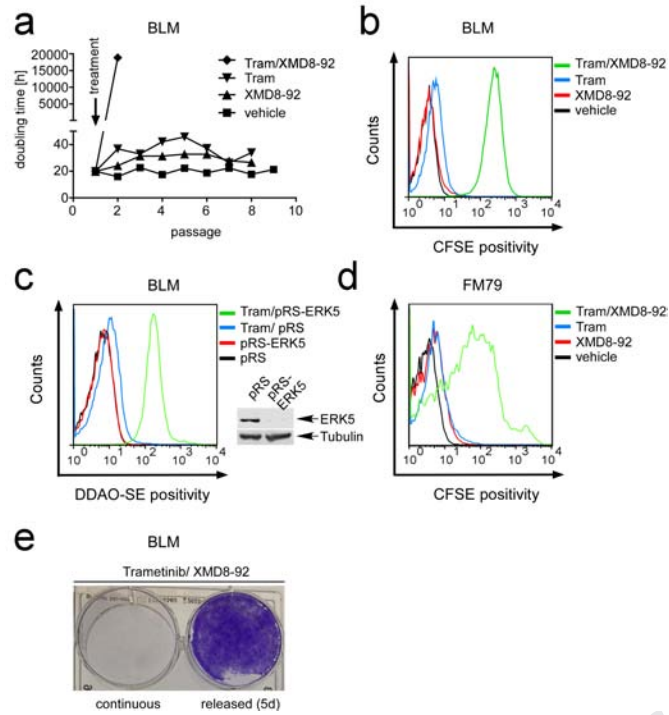
Figure 4. ERK5 activation results in nuclear accumulation of KLF2. (a, b) Immunofluorescence staining, showing KLF2 localization in BLM (a), or FM79 (b) cultured in absence (vehicle) or presence of trametinib, XMD8-92 or a XMD8-92/trametinib combination for 48h (BLM) or 24h (FM79), respectively. Scale bar: 50 μ m. (c) Representative immunohistochemical staining of a FFPE specimen from a human NRAS-Q61K-mutant primary melanoma (MSa001, *top*) or an NRAS-Q61R-mutant melanoma metastasis (MS0188_1, *bottom*) revealing nuclear KLF2 staining within the tumor tissue. *Left*: stitched microscopic large image (LI). *Right*: Higher magnification of the indicated regions. Images were recorded using a 10x (*left*) or 60x (*right*) objective, respectively. Scale bar: 25 μ m.

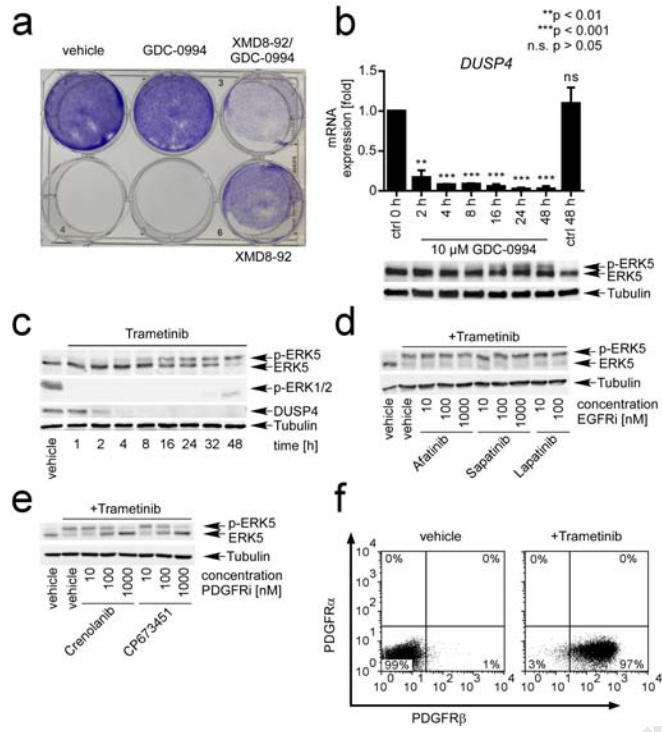
Figure 5. Co-inhibition of MEK1/2 and ERK5 suppresses tumor growth of NRAS-mutant human melanoma xenografts. (a-d) Tumor growth of xenografted human BLM (a, b) or FM79 (c, d) in immune-deficient NOD/SCID mice. Treatment was initiated when tumor volumes reached ~ 150 mm³, and mice treated daily by interperitoneal injection for 14 days as indicated (daily doses: trametinib: 0.1 mg/kg body weight, XMD8-92: 100 mg/kg body weight). (a, c) Kinetics of tumor growth over 15 days. Shown are mean tumor volumes \pm

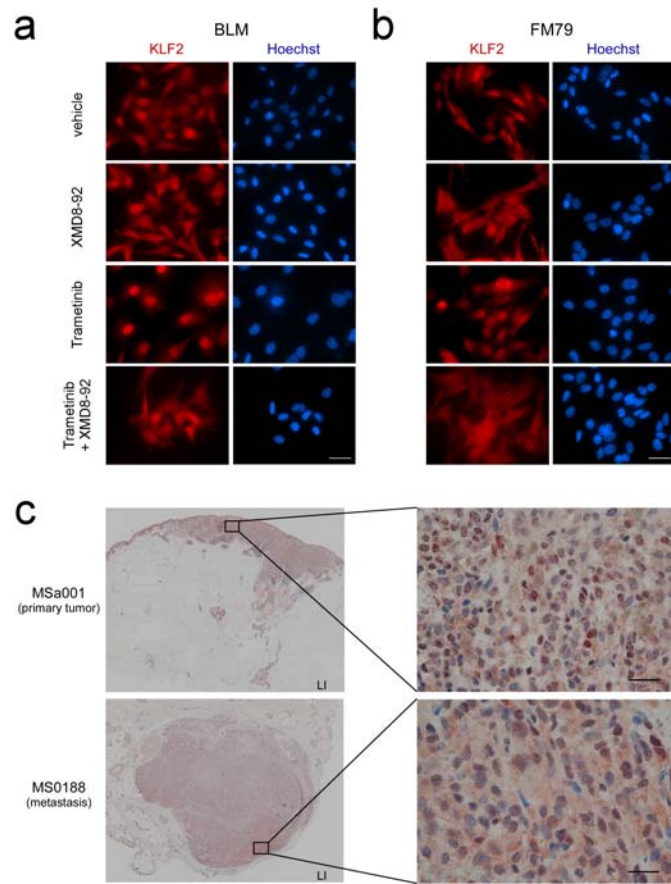
SEM per treatment group. **(b, d)** Representative images of tumor sizes at the experimental endpoint. **(e)** Representative microscopic images, illustrating expression level and localization of KLF2 protein in the tumor tissue of the differently treated BLM (*top*)- or FM79 (*bottom*)-xenografts. Scale bar: 50 μm .

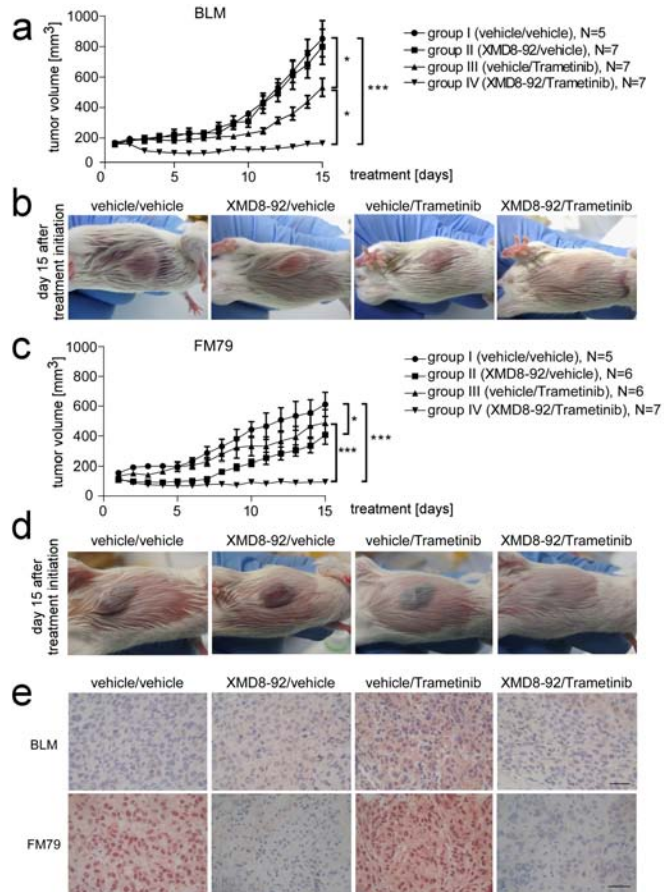
Journal Pre-proof

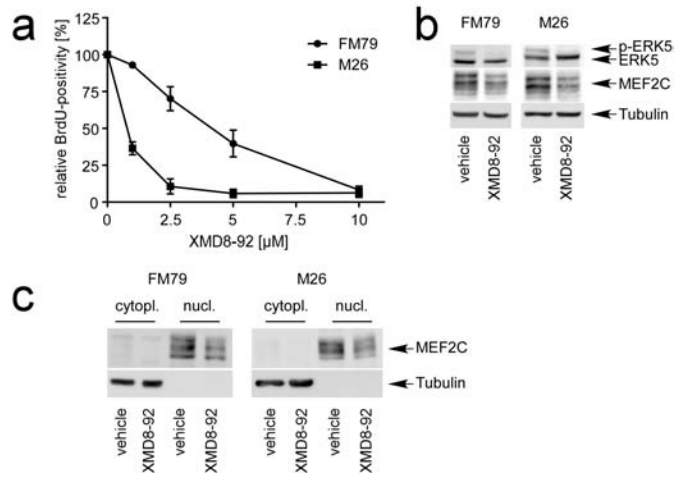




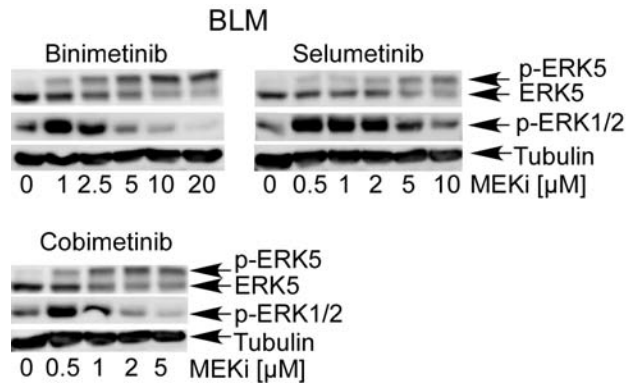


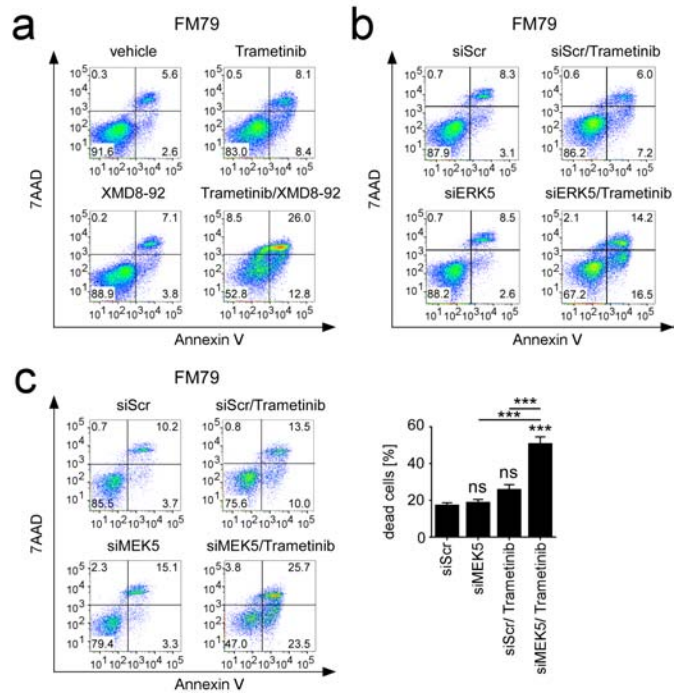


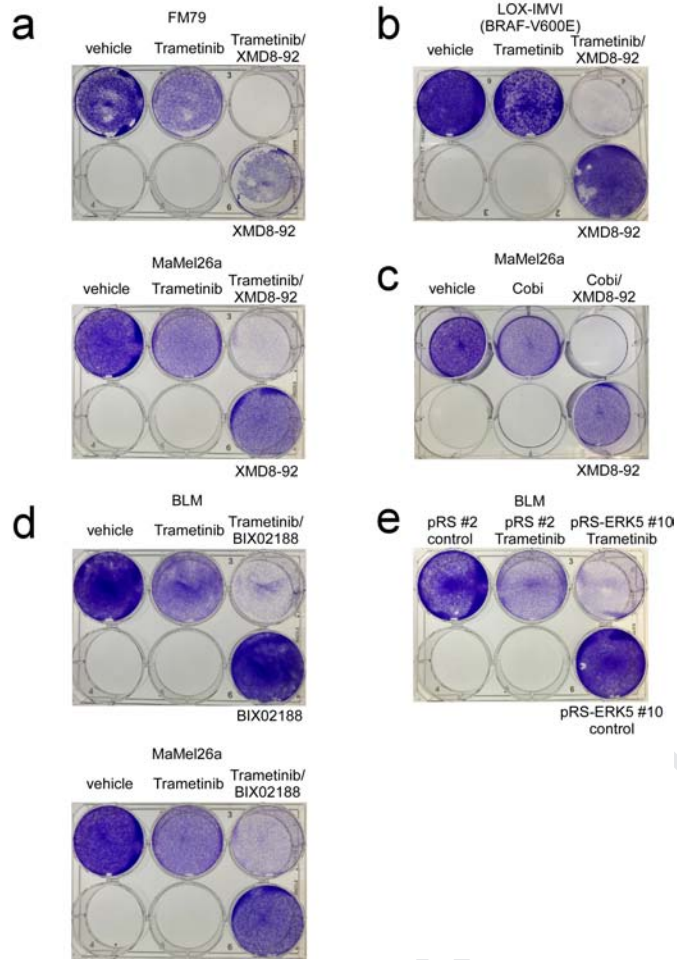


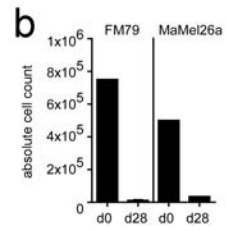
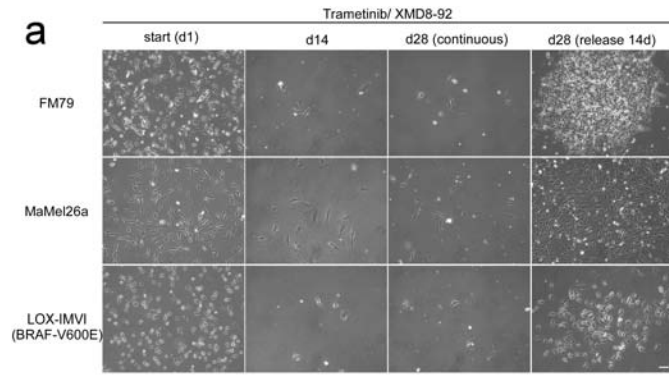


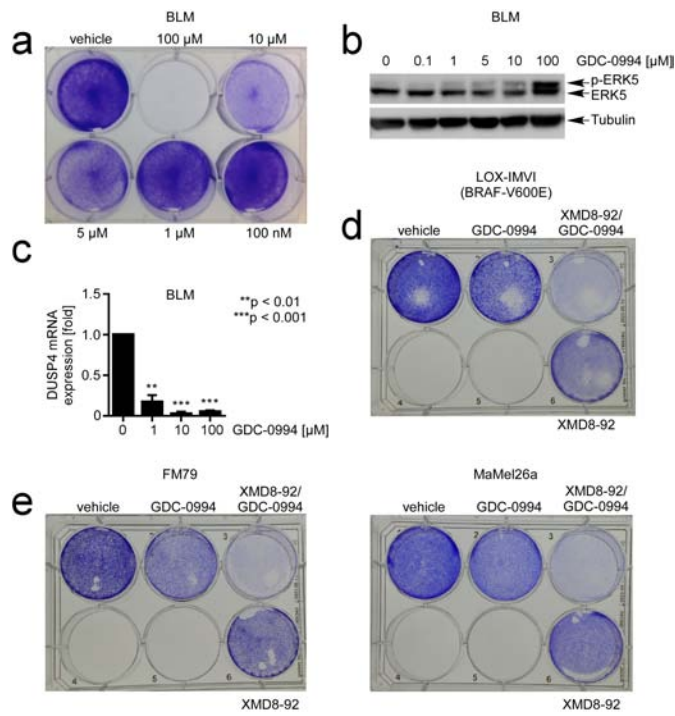
Journal Pre-proof

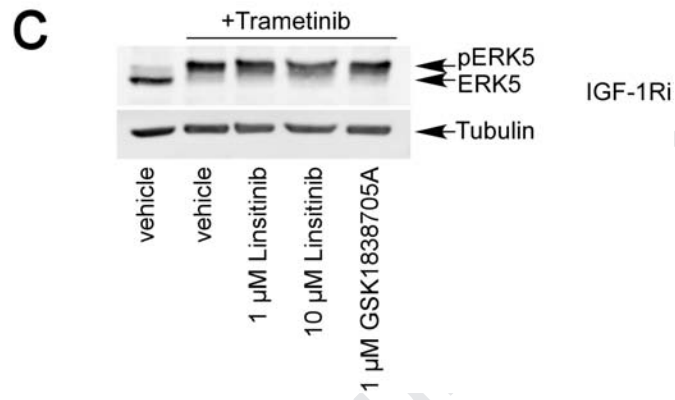
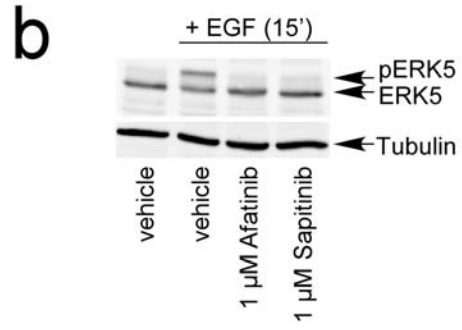
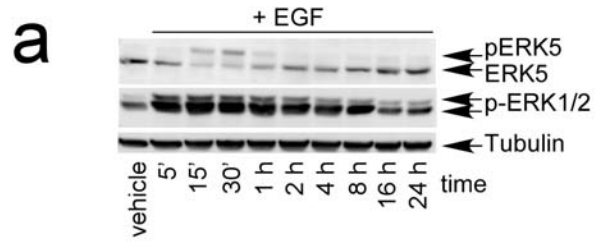


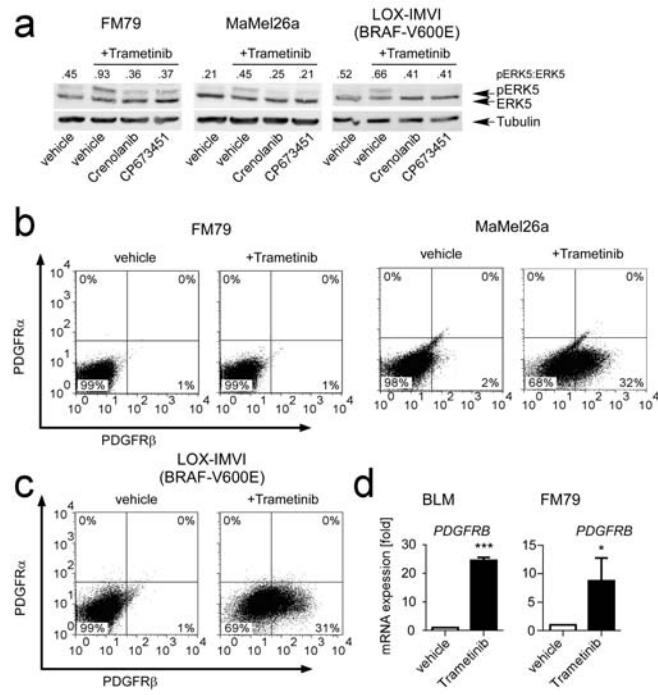


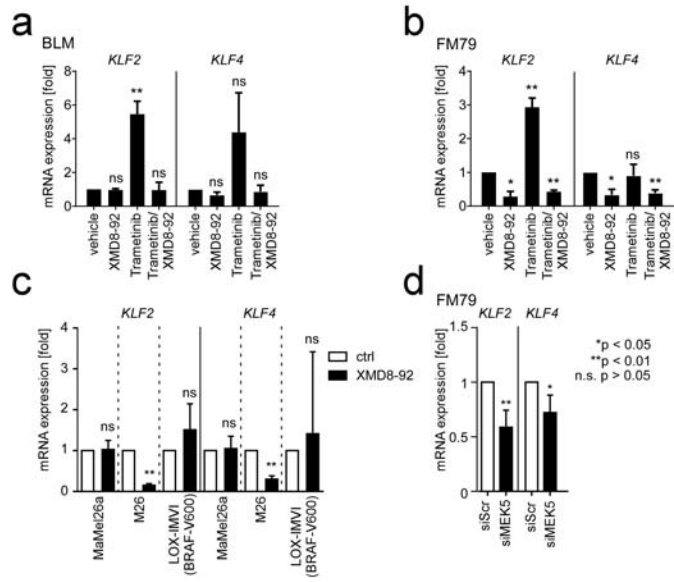












Pat. ID	NRAS-Mutation	Type	Localisation	Total N+C or N
MS0112	Q61K	M	C	6/18 = 30 %
MS0188_1	Q61R	M	N	
MS0105	Q61R	M	N (+C)	
MS0185_2	Q61K	M	C	
MS0198	Q61R	M	C	
MS0188_2	Q61R	M	N+C	
MS0203	Q61K	M	C	
MS0185_3	Q61K	M	N	
MS0150_2	Q61R	M	N	
MS0210	Q61R	M	C	
MS0216_a	Q61K	M	C (+ single N)	
MS0141	Q61R	M	C (+ single N)	
MS0155	Q61K	P	C	
MS0215_1	Q61R	P	C (+ single N)	
MS0349_1	Q61K	P	-	
MS0181	Q61K	P	C (+ single N)	
MS0142	Q61K	P	C	
Msa001	Q61K	P	N	

Supplementary Table 1.

- = no detectable staining; C= cytoplasmic (>50% of stained cells);
N= nuclear (>50% of stained cells); C+N (~1:1 ratio nuclear and
cytoplasmic staining) P= Primary tumor, M= metastasis

SUPPLEMENTARY INFORMATION

Adam et al., **Efficient suppression of NRAS-driven melanoma by co-inhibition of Erk1/2 and Erk5 MAPK pathways**

Contents:

Supplementary Methods

Supplementary Figures 1-9

Supplementary Table 1

Supplementary References

SUPPLEMENTARY METHODS

Generation of shRNA-expressing single clones

For generation of BLM single cell clones stably expressing an empty shRNA expression vector or small hairpin RNA (shRNA) against ERK5, BLM were cotransfected with an excess of an ERK5 shRNA-expressing retroviral vector (pRetro Super puro (pRS) ERK5) (Ohnesorge et al., 2010) in combination with a spectrin-GFP expression plasmid using nucleofection (Lonza). Positively transfected cells were selected by means of a puromycin resistance gene expressed from the pRS backbone and outgrowing GFP-positive single cell clones picked for further expansion and analysis of effective ERK5 protein knockdown by immunoblot prior use for the respective experiments.

Crystal violet assays

For analysis of short-term drug/shRNA effects on proliferation/cytotoxicity by crystal violet staining, the different melanoma cell lines were seeded at densities between $5-8 \times 10^4$ cells/well onto 6-well plates, and treated with the respective pharmacological inhibitors at the following day. When controls approached confluency (~3-6 days after seeding), wells were washed twice with PBS, stained for 60 min with crystal violet staining solution (0.5% crystal violet, 20% methanol in H₂O) and rinsed three times with tap-water. Subsequently, plates were air-dried and results documented by photography.

BrdU incorporation assays

BrdU incorporation assays were performed as described (Czymai et al., 2010). Briefly, 1.2×10^5 M26 or 1.8×10^5 FM79 melanoma cells were seeded onto 6 cm dishes and the following day treated with XMD8-92 or vehicle for 48 h. At day 3, cells were pulsed for 30 min with 1 μ M BrdU and attached cells and culture supernatants were harvested together and pooled for pelletation. Cell pellets were rinsed twice with ice-cold PBS and fixed overnight in 70%

ethanol. Thereafter, nuclei were isolated and processed for flow cytometric analysis of S-phase distribution by co-staining with a fluorescein isothiocyanate-coupled anti-BrdU antibody (Becton Dickinson) and the DNA dye propidium iodide (PI; 10 µg/ml PI, 0.25 mg/ml RNase in PBS).

siRNA transfections and sequences

BLM or FM79 were seeded at densities of 1.5×10^5 or 2.2×10^5 /well into 6-well plates, and the following day transfected with single validated siRNAs or a pool of two different siRNAs at a final concentration of 10 nM using Lipofectamine® RNAiMAX (ThermoFisher, Darmstadt, Germany) according to the manufacturer's guidelines. 24 h post transfection, medium was replaced, and cells were stimulated with the indicated pharmacological inhibitors for 72 h in the different assays. Knockdown efficiencies were routinely validated by qPCR or immunoblot, respectively. The following synthetic and functionally verified siRNA molecules were used:

siERK5: 5'-GGCUCGGCUUGGAUUAUUCdTdT-3' (MWG) and s11149 Silencer® Select siRNA, 4390824 (ThermoFisher, Darmstadt, Germany); siMEK5: SI00300713 (Qiagen, Hilden, Germany)

A scrambled (Scr) siRNA with sequence 5'-UUCUCCGAACGUGUCACGudTdT-3' (Eurofins Genomics, Ebersberg, Germany) showing no homology to any known gene served as negative control.

Long-term proliferation analysis by cell doubling time analysis and CFSE/DDAO-SE live dye labelling

For long-term analysis of cell proliferation by cell doubling analysis, the different melanoma cell lines were seeded on 10 cm dishes at fixed densities between 2 to 7.5×10^5 cells, depending on the proliferation rate of the respective cell line. The following day, cells were

treated with the indicated inhibitors for a period of four weeks. When cells reached confluence, cells were detached, counted and reseeded at the initial density onto new 10 cm dishes. Passage numbers were documented and cell doubling times calculated according to the formula $\text{cultivation time [h]} / (\log_2 N(t) - \log_2 N(0))$, with $N(0)$ denoting the initially seeded cell number and $N(t)$ the cell count determined at the experimental endpoint, respectively.

As alternative method to follow cell divisions over time we labelled cells with the cell-activated fluorescent live dyes CFSE (carboxyfluorescein diacetate succinimidyl ester) or DDAO-SE (decyl dimethyl amine oxide succinimidyl ester/Cell Trace™ Far Red) (ThermoFisher, Darmstadt, Germany) and determined fluorescence intensity in response to the different treatments by flow cytometry. Fluorescence intensity proportionally decreases during proliferation as dyes are equally distributed among daughter cells during mitosis but is retained in cell cycle-arrested cells, allowing analysis of cell cycle arrest/division. Briefly, the different melanoma cell lines were detached at the start of the experiment and labelled with 5 μM of the respective dye as suggested by the manufacturer's instructions. Labelled cells were distributed into separate dishes and upon attachment subjected to the respective treatments for a period of 14 days. Medium was replaced by fresh inhibitor-supplemented growth medium twice per week and cells passaged when they approached confluence. Division-dependent loss of fluorescence intensity was then quantified by analysis of logarithmic green (CFSE) or far-red (DDAO-SE) fluorescence by flow cytometry, respectively.

Immunofluorescence and immunohistochemistry

For KLF2 detection by immunofluorescence, melanoma cells were grown on coverslips, fixed with 4% paraformaldehyde (PFA), pH 7.4 and permeabilized by incubation in 0.1% Triton X-100 solution. Subsequently, blocking was performed by applying 4% FCS for 60 min, followed by incubation with KLF2 antibody (1:25 in 4% FCS/PBS) for another 60 min at

room temperature. For visualization, an anti-rabbit secondary antibody coupled to Alexa568 fluorescent dye (ThermoFisher, Darmstadt, Germany) was used. Nuclei were counterstained with Hoechst33342 (Sigma Aldrich, Munich, Germany) and samples mounted using mounting medium from IBIDI (Gräefeling, Germany).

For immune histochemical staining of KLF2 on FFPE tumor samples, antigen was retrieved by incubation of the de-paraffinized sections with Target Retrieval Solution (Dako, Hamburg, Germany) at pH 6.0, followed by blocking with 4% FCS for 60 min at room temperature. Sections were incubated overnight with a 1:100 dilution of KLF2 antibody in 4% FCS/0.1% Tween-20/TBS in a humidified chamber at 4°C. For detection, the REAL™ Detection System, alkaline phosphatase/RED (Dako, Hamburg, Germany) was applied according to the manufacturer's protocol. Slides were counterstained with Mayer's hematoxylin (Dako, Hamburg, Germany) and mounted with Aquatex® (Merck, Darmstadt, Germany). Photographs were taken using a Nikon Ti-E motorized stage fluorescence microscope equipped with color and monochrome cameras and a solid state fluorescence light source. Whole tumor images were generated by automated stitching of overlapping image tiles using NIS Elements AR software (Nikon, Düsseldorf, Germany).

Nuclear and cytoplasmic extractions

For preparation of nuclear and cytoplasmic extracts, the different melanoma cell lines were seeded at densities between $3.5 - 7.5 \times 10^5$ onto 10 cm dishes and treated with the respective inhibitors the following day for 48 h. Cells were harvested by trypsinization, washed twice with ice cold PBS and cell pellets resuspended in 200 µl buffer A (10 mM HEPES pH7.9, 10 mM KCl, 0.1 mM EGTA, 0.1 mM EDTA, freshly supplemented with 1mM DTT and 0.5 mM PMSF). After 15 min incubation at 4°C cells were pressed through a 1 ml syringe with a 26G3/8 (0,45x10) needle on ice and centrifuged for 5 min at 5000 rpm at 4°C in a microcentrifuge. Supernatants containing the cytoplasmic fractions were separated and

centrifuged for 10 min at 14000 rpm/4°C in a microcentrifuge to remove nuclear contaminants. Remaining pellets containing the nuclear fraction were washed twice with 500 µl buffer A by gentle inversion, followed by centrifugation at 5000 rpm/4°C (5 min) in a microcentrifuge. Nuclear extracts were then prepared by resuspension of the pellets in 50 µl buffer B (20 mM HEPES pH7.9, 0.4 M NaCl, 1 mM EGTA, 1 mM EDTA, freshly supplemented with 1mM DTT and 1 mM PMSF) and incubation at 4°C on a rocker for 15 min. Insoluble debris was removed by centrifugation (10 min, 14000 rpm at 4°C), and equal protein amounts of nuclear and cytoplasmic extracts loaded onto SDS-PAGE gels for analysis of localization of the respective proteins by immunoblot.

Densitometric analysis of immunoblots.

Densitometric analysis of phosphorylated and unphosphorylated ERK5 bands was performed on the original 16 bit Tiff image exposures of the immunoblots generated by a camera-based electronic ECL imaging system (GE Healthcare, Freiburg, Germany) using Amersham™ ImageQuant TLv8.1.0.0 analysis software. Data were each represented as ratio of the obtained values for phosphorylated ERK5/unphosphorylated ERK5 to judge the degree of ERK5 phosphorylation for the respective cell lines and treatments.

Statistical analysis

At least three individual experiments were averaged and error bars calculated to indicate the ± s.d. For normalized data, one-sample *t* tests with posthoc Bonferroni-Holm multiplicity correction were employed. Multiple groups were analyzed by one-way or two-way analysis of variance (ANOVA) followed by adequate multiplicity correction. Adjusted p-values of <0.05 were considered significant and marked by asterisks. All statistical calculations were performed using GraphPad Prism 6 software.

SUPPLEMENTARY REFERENCES

Czymai T, Viemann D, Sticht C, Molema G, Goebeler M, Schmidt M. FOXO3 modulates endothelial gene expression and function by classical and alternative mechanisms. *J Biol Chem* 2010;285:10163-78.

Ohnesorge N, Viemann D, Schmidt N, Czymai T, Spiering D, Schmolke M, et al. Erk5 activation elicits a vasoprotective endothelial phenotype via induction of Kruppel-like factor 4 (KLF4). *J Biol Chem* 2010;285:26199-210.

Journal Pre-proof